

# Current density functional theory of spontaneously magnetised solids

H. Ebert and Marco Battoletti

*Institute for Physical Chemistry, University of Munich, Theresienstr. 37, D-80333 München, Germany*

E. K. U. Gross

*Institute for Theoretical Physics, University of Würzburg, Am Hubland, D-97074 Würzburg*

(July 8, 1997)

The first application of current density functional theory (CDFT) to spontaneously magnetised solids is presented. We show that non-relativistic CDFT without spin-orbit coupling does not lead to finite orbital currents. In accordance with experiment an enhancement of the spin-orbit induced orbital magnetic moment is found for the ferromagnets Fe and Co while for Ni only a minor change was found compared to a plain calculation done within spin density functional theory (SDFT).

Ms number LB6710. PACS numbers: 71.15.Mb, 71.15.Rf, 71.20.Be, 75.10.Lp

Current-density functional theory (CDFT)<sup>1-3</sup> is a powerful tool to treat interacting many-body systems in magnetic fields of arbitrary strength. The response of atoms and molecules<sup>4</sup> to magnetic fields has been successfully described on the basis of CDFT, electron-hole droplets<sup>5</sup> and the Wigner crystallisation<sup>6</sup> in strong magnetic fields have been treated and, most recently, the two-dimensional electron gas in the quantum Hall regime<sup>7</sup> has been studied. The aim of the present Letter is to investigate the orbital magnetic moment of spontaneously magnetised solids on the basis of CDFT.

Although principally designed for systems in strong magnetic fields, CDFT can also be applied in situations where currents are present without external magnetic fields. The motivation for doing so is similar to the motivation for using spin density functional theory (SDFT) rather than ordinary DFT to describe spin-polarised systems in absence of external magnetic fields: The Kohn-Sham (KS) orbitals of ordinary DFT only yield the correct ground-state density of the system; spin-related quantities, in particular the spin magnetisation itself, are hard to calculate in ordinary DFT because these quantities are highly non-local functionals of the density. The KS orbitals of SDFT, on the other hand, yield the correct density *and* the correct spin magnetisation. Hence, spin-related observables are easily obtained in SDFT. However, there is no guarantee that the current density resulting from the SDFT KS orbitals is the correct current of the interacting system at hand. This is the point where CDFT comes into play. The KS orbitals of CDFT yield the correct spin densities *and* the correct paramagnetic current densities. Hence one expects that the description of current-related quantities is improved by employing CDFT rather than SDFT.

The spin-orbit induced orbital magnetic moments of spontaneously magnetised solids is often severely underestimated by SDFT calculations.<sup>8</sup> The calculated values are up to 60 % too small compared with experiment. In this Letter we shall demonstrate that this discrepancy is reduced by employing CDFT. Besides that we shall investigate whether the effective vector potential of CDFT alone (i.e. without spin-orbit coupling) can sustain a fi-

nite orbital current in the absence of external magnetic fields.

The central statement<sup>1-3</sup> of CDFT is a HK-type theorem stating that the many-body ground-state wave function is uniquely determined by the ground-state spin densities  $n_\sigma$  and the spin-resolved paramagnetic current densities  $\vec{j}_{p,\sigma}$ . Hence any ground-state expectation value can formally be considered as a functional of these densities. The corresponding KS equations read as follows:<sup>1-3</sup>

$$\left( -\frac{\hbar^2}{2m} \vec{\nabla}^2 - \frac{i\hbar e}{2mc} \left[ \vec{A}_{xc,\sigma}(\vec{r}), \vec{\nabla} \right]_+ + V_H(\vec{r}) + V_{xc,\sigma}(\vec{r}) \right) \varphi_{i,\sigma}(\vec{r}) = \epsilon_{i,\sigma} \varphi_{i,\sigma}(\vec{r}), \quad (1)$$

where  $V_H$  is the Hartree potential. The exchange-correlation scalar and vector potentials,  $V_{xc,\sigma}$  and  $\vec{A}_{xc,\sigma}$ , respectively, are given by:<sup>1,2</sup>

$$V_{xc,\sigma}(\vec{r}) = \frac{\delta E_{xc}[n_\sigma, \vec{\nu}_\sigma]}{\delta n_\sigma(\vec{r})} \Big|_{\{\vec{\nu}_\sigma\}, n_\sigma} - \frac{e}{c} \vec{A}_{xc,\sigma}(\vec{r}) \frac{\vec{j}_{p,\sigma}(\vec{r})}{n_\sigma(\vec{r})} \quad (2)$$

$$\frac{e}{c} \vec{A}_{xc,\sigma}(\vec{r}) = \frac{1}{n_\sigma(\vec{r})} \vec{\nabla} \times \frac{\delta E_{xc}[n_\sigma, \vec{\nu}_\sigma]}{\delta \vec{\nu}_\sigma(\vec{r})} \Big|_{\vec{\nu}_\sigma, \{n_\sigma\}}. \quad (3)$$

$E_{xc}[n_\sigma, \vec{\nu}_\sigma]$  is the exchange-correlation (xc) contribution to the total energy which, as a consequence of gauge invariance, depends on  $\vec{j}_{p,\sigma}$  only through the so-called vorticity

$$\vec{\nu}_\sigma(\vec{r}) \equiv \vec{\nabla} \times \frac{\vec{j}_{p,\sigma}(\vec{r})}{n_\sigma(\vec{r})}. \quad (4)$$

In practice the xc energy functional needs to be approximated. We have employed the local-vorticity approximation proposed by Vignale and Rasolt<sup>2</sup> for the case of small vorticities:

$$E_{xc}[n_\sigma, \vec{\nu}_\sigma] \approx E_{xc}^{\text{LDA}}[n_\sigma] + \sum_\sigma \int d^3r \frac{m k_{F,\sigma}}{48\pi^2} \left( \frac{\chi_{L,\sigma}}{\chi_{L,\sigma}^0} - 1 \right) |\vec{\nu}_\sigma(\vec{r})|^2, \quad (5)$$

where the Fermi vector  $k_{F,\sigma}$  is determined by the local densities  $n_\sigma$  in the usual way and  $\frac{\chi_{L,\sigma}}{\chi_{L,\sigma}^0}$  is the ratio of the Landau susceptibilities<sup>9</sup> for the interacting and non-interacting homogeneous electron gas, respectively.<sup>10</sup>

The CDFT KS equation (1) differs from the ordinary SDFE KS equation by the appearance of the xc vector potential  $\vec{A}_{xc}$ . This term ensures that the single-particle orbitals resulting from Eq. (1) not only reproduce the spin densities  $n_\sigma$  but also the current densities  $\vec{j}_{p,\sigma}$  of the interacting system of interest. Since the exchange-correlation potential breaks time reversal symmetry it is conceivable that non-relativistic CDFT, i.e. Eq. (1) without additional spin-orbit coupling (SOC), might lead to a finite orbital magnetic moment. To investigate this question we performed a calculation including SOC that led to a finite orbital magnetic moment (see below). Then, starting with this solution, the spin-orbit coupling was switched off. In the subsequent self-consistent iterations the orbital magnetic moment approached zero, demonstrating that the presence of  $\vec{A}_{xc}$  alone cannot sustain a finite orbital magnetic moment.

If spin-orbit coupling is accounted for, the orbital angular momentum is not completely quenched in a solid. Then, since the corresponding orbital current densities enter the above equations (1)–(4) there will be a feedback via the potential terms and changes are expected for all observables as compared to pure relativistic SDFE<sup>11</sup> calculations. Usually, SOC is accounted for in the variational step of a conventional  $\vec{k}$ -space band structure method<sup>12</sup> using a scalar relativistic basis set. As an alternative one may solve the Dirac equation for a spin dependent potential<sup>13</sup> and use the solutions as basis functions for a  $\vec{k}$ -space method<sup>14</sup> or within multiple scattering theory.<sup>15,16</sup> The latter approach is adopted here. In principle, the corresponding Dirac-Kohn-Sham equation<sup>17</sup> has to be solved accordingly. However, for this relativistic framework, no current-dependent exchange-correlation functionals are available to date. We therefore take resort to a hybrid scheme where only the kinetic energy is calculated in a fully relativistic way whereas the potential terms are treated consistently to first order in  $1/c$ , i.e., the following equation is used:

$$\left( -i\hbar c \vec{\alpha} \cdot \vec{\nabla} + \beta m c^2 + V_{\text{eff}}(\vec{r}) + \beta \sigma_z \cdot B_{\text{eff}}(\vec{r}) - \frac{i\hbar e}{2mc} \beta \sum_{\sigma} \left[ \vec{A}_{xc,\sigma}(\vec{r}), \vec{\nabla} \right]_{+} P_{\sigma} \right) \Psi_i(\vec{r}) = \epsilon_i \Psi_i(\vec{r}). \quad (6)$$

We note that this equation not only contains the potential terms of Eq. (1) to first order in  $1/c$ , it also leads to the conventional SOC term when expanded to second order in  $1/c$ .<sup>18</sup> The scalar potential terms  $V_{\text{eff}}$  and  $B_{\text{eff}}$  stand for the average and difference, respectively, of the two spin-dependent potentials  $V_H + V_{xc,\sigma}$ . Since in the present formalism  $\vec{A}_{xc,\sigma}$  is defined in a spin-dependent way the spin-projection operator  $P_{\sigma} = \frac{1 \pm \beta \sigma_z}{2}$  appears in

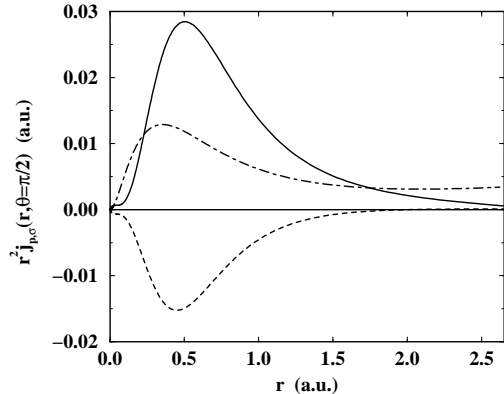


FIG. 1. Valence band part of the polar component of the spin-resolved paramagnetic current density  $j_{p,\sigma}(r, \theta = \pi/2)$  for Fe (in atomic units). The full and dashed lines give the minority and majority part, respectively. In addition a representative radial wave function for d-electrons is given by a dashed-dotted line.

addition to  $\left[ \vec{A}_{xc,\sigma}(\vec{r}), \vec{\nabla} \right]_{+}$  in Eq. (6).

The scheme described above has been implemented by applying appropriate extensions to a spin polarised relativistic Korringa-Kohn-Rostoker-Green's function (SPR-KKR-GF) band structure program working in the atomic sphere approximation (ASA) as well as to corresponding routines for the core states. Within the Wigner-Seitz sphere the particle density  $n_\sigma$  was taken to be spherically symmetric. The current density  $\vec{j}_{p,\sigma}$ , on the other hand, was taken to be rotationally symmetric with the symmetry axis pointing along the magnetisation, which in turn was fixed parallel to the crystallographic z-axis. This means that  $\vec{j}_{p,\sigma}$  is everywhere parallel to the polar unit vector  $\vec{e}_\theta$  and depends only on the spherical coordinates  $r$  and  $\theta$ . For that reason the resulting exchange-correlation vector potential  $\vec{A}_{xc,\sigma}$  is also parallel to  $\vec{e}_\theta$  and rotationally symmetric. This has the important consequence that the coupling term in Eq. (6) causes no further reduction in symmetry compared to a conventional spin polarised relativistic calculation. Furthermore, because of this property, one need not distinguish between left and right hand solutions of the Dirac equation (6) in setting up the Green's function.<sup>19</sup> Further technical details will be given in a forthcoming publication.<sup>20</sup>

In the following we present results for the elemental ferromagnets bcc-Fe, fcc-Co and fcc-Ni, obtained from CDFT in combination with the modified SPR-KKR-GF method. As mentioned above the primary source for the paramagnetic current density  $\vec{j}_{p,\sigma}$  is the SOC. Fig. 1 shows for bcc-Fe the valence band part of this central quantity of CDFT. An angular momentum decomposition of  $\vec{j}_{p,\sigma}$  reveals that – as one expects – it is nearly exclusively due to the d-electrons. Accordingly, its radial distribution is closely linked to the corresponding radial

wave functions. As can be seen both spin-parts  $\vec{j}_{p,\sigma}$  are of opposite sign and differ in a pronounced way in magnitude. Connected with  $\vec{j}_{p,\sigma}$  are corresponding orbital angular momenta  $\langle l_z \rangle_\sigma$  that in turn give rise to the orbital magnetic moment  $\mu_{\text{orb}} \approx \mu_B \sum_\sigma \langle l_z \rangle_\sigma$  which is obviously dominated by its minority spin contribution.<sup>21</sup> There is a rather appreciable contribution to  $\vec{j}_{p,\sigma}$  due to the core electrons. These have not been included in Fig. 1 because the contributions for different spin character nearly cancel each other. The resulting total core contribution to the orbital magnetic moment vanishes exactly. However, since the spatial distribution of the currents themselves differ slightly there results a small but finite orbital contribution to the hyperfine field.<sup>22</sup>

The valence band contribution to the exchange-correlation vector potential  $\vec{A}_{\text{xc}}$  derived for bcc-Fe from Eq. (3) is shown in Fig. 2 for  $\theta = \pi/2$ . Obviously,  $\vec{A}_{\text{xc}}$

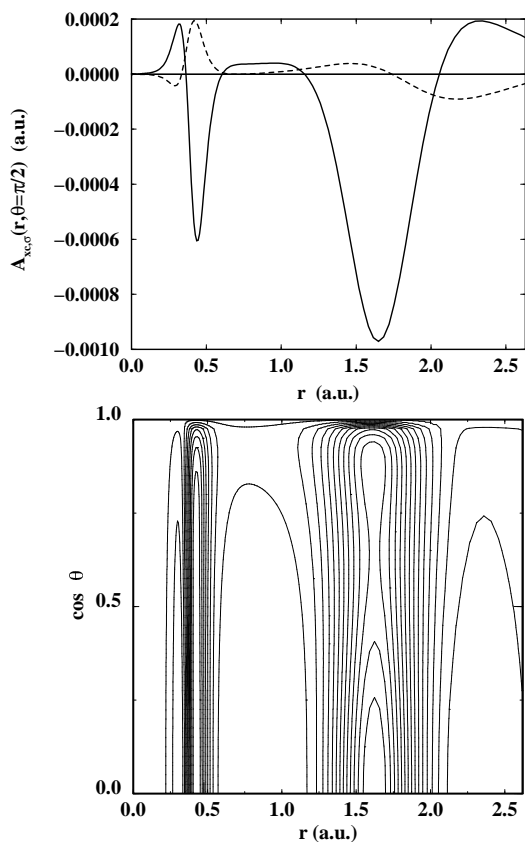


FIG. 2. Valence band part of the polar component of the spin-dependent exchange-correlation vector potential  $A_{\text{xc},\sigma}(r, \theta)$  for Fe (in atomic units). In the upper part the full and dashed lines give the potential for minority and majority character, respectively, for  $\theta = \pi/2$ . In the lower part, the potential for the minority character is shown as a function of  $r$  and  $\theta$ .

possesses a rather complex radial variation that shows no direct and simple relationship to the current density

distribution. As for  $j_{p,\sigma}$ , there are quite appreciable contributions to  $\vec{A}_{\text{xc}}$  from the core states in the region near the nucleus. However, suppression of these contributions has hardly any influence on the orbital magnetic moment  $\mu_{\text{orb}}$  (see below). For that reason one can conclude that the variation of  $\vec{A}_{\text{xc}}$  in the region between  $r \approx 1$  a.u. (Bohr radius) and the Wigner-Seitz-radius is most important for  $\mu_{\text{orb}}$ . This implies that for calculating  $j_{p,\sigma}$  the core states can be ignored and that the latter can be treated within conventional SDFT.

From the lower panel of Fig. 2 one can see that  $\vec{A}_{\text{xc}}$  depends to some extent on the azimuthal angle  $\theta$ . To simplify the solution of the radial Dirac equations corresponding to Eq. (6) the average of  $\vec{A}_{\text{xc}}$  with respect to  $\theta$  has been used. Via this procedure, the term  $\frac{e}{2mc} [\mathbf{A}_{\text{xc}}(r, \theta), \hat{\mathbf{p}}]_+$  in Eq. (1) is replaced by  $\frac{e}{2mc} \frac{\vec{A}_{\text{xc}}}{r \sin \theta} \hat{l}_z$  where  $\hat{l}_z$  denotes the z-component of the orbital angular momentum operator. This term is similar in form to the expression  $f^{\text{OP}}(r) \hat{l}_z$  recently obtained within the extended orbital-polarisation (OP) formalism.<sup>8</sup> The OP-approach was originally introduced by Brooks and coworkers<sup>23</sup> in a way to be used within a variational band structure method. This allowed to add to the Hamiltonian matrix a perturbational term that is borrowed from atomic Hartree-Fock theory and that is meant to account for Hund's second rule i.e. to maximise the orbital angular momentum. Obviously the physical picture behind the OP-formalism is quite different from the CDFT as used here. While for the former case one tries to account in an approximate way for intra-atomic correlations the vector potential occurring within CDFT is due to diamagnetic contributions to the exchange-correlation energy of the electron gas.

Application of the SPR-KKR method in the framework of relativistic SDFT leads to 2.27, 1.57 and 0.57  $\mu_B$  for the spin magnetic moments of bcc-Fe, fcc-Co and fcc-Ni, respectively. These values agree within a few percent with experiment and change by less than 1% if the OP- or the CDFT-formalism is adopted. As Fig. 3 shows, quite pronounced deviations from experiment occur if the orbital magnetic moment  $\mu_{\text{orb}}$  is calculated using the plain SPR-KKR. This discrepancy is nearly removed in the OP-formalism<sup>8</sup> which has the effect of enhancing the spin-orbit induced orbital moments. This enhancement is also found in our CDFT calculations, although it seems somewhat too small for Fe and – more pronounced – for Co. There are several possible reasons for this: First of all one has to note that Eq. (5) based on linear response theory has only a certain range of applicability which is definitely left for the systems investigated here. Furthermore  $\chi_{L,\sigma}/\chi_{L,\sigma}^0$  is available so far only for the non-spin-polarised electron gas. Finally, one may expect that the various technical approximations made to implement the CDFT have their influence on the final result, making a full potential treatment desirable.

In summary, the CDFT has been applied for the first time to spontaneously magnetised solids demonstrating

